tvst

Article

Subretinal Pigment Epithelium Illumination Combined With Focal Electroretinogram and Visual Acuity for Early Diagnosis and Prognosis of Non-Exudative Age-Related Macular Degeneration: New Insights for Personalized Medicine

Maria Cristina Savastano[1,2,*], Benedetto Falsini[1,2,*], Silvia Ferrara[1,2], Alessandra Scampoli[1,2], Marco Piccardi[1,2], Alfonso Savastano[1,2], and Stanislao Rizzo[1–3]

[1] Ophthalmology Unit, Fondazione Policlinico Universitario A. Gemelli IRCCS, Rome, Italy
[2] Università Cattolica del Sacro Cuore, Rome, Italy
[3] Consiglio Nazionale delle Ricerche, Istituto di Neuroscienze, Pisa, Italy

Correspondence: Alfonso Savastano, Fondazione Policlinico Universitario A Gemelli, Largo A. Gemelli 8, 00168 Rome, Italy. e-mail: alfonso.savastano@policlinicogemelli.it

Received: September 26, 2021
Accepted: December 21, 2021
Published: January 25, 2022

Keywords: non-exudative age-related macular degeneration; outer retina; personalized medicine; retinal pigment epithelium; visual acuity; focal electroretinogram

Citation: Savastano MC, Falsini B, Ferrara S, Scampoli A, Piccardi M, Savastano A, Rizzo S. Subretinal pigment epithelium illumination combined with focal electroretinogram and visual acuity for early diagnosis and prognosis of non-exudative age-related macular degeneration: New insights for personalized medicine. Transl Vis Sci Technol. 2022;11(1):35, https://doi.org/10.1167/tvst.11.1.35

Purpose: To evaluate the correlation between functional visual acuity and focal electroretinograms (fERGs) and morphological abnormalities in the retinal pigment epithelium and outer retinal atrophy (RORA) assessed by subretinal illumination (SRI) parameter at optical coherence tomography (OCT) examinations as signs of early disease in early and intermediate non-exudative age-related macular degeneration (ne-AMD).

Methods: One hundred forty-one eyes of 74 patients were retrospectively evaluated. A subgroup of patients (34/74) had a follow-up of at least 1 year. The study included both cross-sectional and longitudinal analyses. All eyes were assessed by OCT to measure the macular outer nuclear layer thickness, extent of ellipsoid zone interruption, absence or presence of drusen/reticular pseudodrusen in the foveal and perifoveal fields, and the SRI area closest to the fovea. Additionally, fERGs were performed.

Results: In the cross-sectional analysis, visual acuity and fERG amplitude were correlated ($P < 0.01$) with the SRI area. The fERG amplitude was correlated ($P < 0.01$) with the extent of ellipsoid zone interruption and tended to be lower in reticular pseudodrusen compared with drusen. In the longitudinal analysis, fERG amplitudes and outer retinal thickness tended to decrease on average by 15% and 18%, respectively, after 1 year of follow-up. The baseline RORA area, but not fERG amplitude or visual acuity, significantly predicted with 77% accuracy ($P < 0.01$) morphological deterioration, which was determined by an increase in the RORA area after 1 year.

Conclusions: Functional visual acuity and its morphological correlations can be assessed in early and intermediate ne-AMD eyes. SRI, as a result of RORA, is a potential predictor of ne-AMD progression in a short-term follow-up.

Translational Relevance: SRI assessment, an objective method to measure RORA, is a potential biomarker for non-exudative AMD progression.

Introduction

Age-related macular degeneration (AMD) is one of the leading causes of worldwide vision loss.[1] The diagnostic signs of early and intermediate non-exudative AMD (ne-AMD) are based on specific sizes, types, and locations of drusen and anomalies of the retinal pigment epithelium (RPE). Drusen are considered the hallmark lesions of aging, and they are

Copyright 2022 The Authors

This work is licensed under a Creative Commons Attribution-NonCommercial-NoDerivatives 4.0 International License.

Downloaded from tvst.arvojournals.org on 04/22/2022

classified as different types. Hard and soft drusen consist of sub-RPE deposits of amyloid, cholesterol, and lipoproteins. Reticular pseudodrusen represent subretinal drusenoid deposits that are similar to drusen in composition but with higher concentrations of unesterified cholesterol, vitronectin, and, in contrast to drusen, photoreceptor pigments such as opsins.[2,3] The Age-Related Eye Disease Study (AREDS) determined that large drusen in the central macula and pigment changes identified on color fundus photography indicate an increased risk of macular degeneration.[3] Recently, multimodal imaging, including optical coherence tomography (OCT), has identified reticular pseudodrusen as being a macular feature of the evolution of geographic atrophy; other signs of progression include increased drusen volume, decreased internal reflectivity of drusen (identified as calcified drusen), and intraretinal hyperreflective foci.[4–7] Several classifications are based on drusen characteristics and the alterations of epithelial pigmentation to differentiate early and intermediate ne-AMD. One of the most recent is the evidence-based clinical classification system described by Ferris et al.,[8] which is based on fundus lesions assessed within 2 disc diameters of the fovea in persons older than 55 years. According to this classification, the presence and dimension of drusen and pigment abnormalities (hyper- or hypopigmentation) are criteria to establish ne-AMD stage. Early ne-AMD is characterized by medium (<63 and <125 µm) drusen and no pigmentary abnormalities, whereas intermediate ne-AMD is identified by the presence of large (>125 µm) soft drusen. The advanced stages of ne-AMD are defined by the presence of geographic atrophy.[8] Recently, the Classification of Atrophy Meetings program suggested a new consensus nomenclature for the various AMD stages based on the use of high axial resolution OCT to detect lesions more accurately even before they become clinically visible on color fundus photography.[9]

Guymer et al.[10] defined incomplete or complete retinal pigment epithelium and outer retinal atrophy (iRORA or cRORA) based on OCT-specific findings, such that iRORA is characterized by (1) a region of signal hypertransmission into the choroid not exceeding 250 µm; (2) a corresponding zone of attenuation or disruption of the RPE, with or without persistence of basal laminar deposits; and (3) evidence of overlying photoreceptor degeneration, including subsidence of the inner nuclear layer and outer plexiform layer, presence of a hyporeflective wedge in the Henle fiber layer, thinning of the outer nuclear layer (ONL), interruption of the external limiting membrane, or segmentation of the ellipsoid zone (EZ). When the RORA involves more than 250 µm, then it is referred to as cRORA, which corresponds to geographic atrophy.

Retinal sensitivity is reported to be reduced in the early ne-AMD stage.[11] Central retinal function properties, as evaluated by focal electroretinogram (fERG), decreased in eyes before visual acuity, and funduscopic changes were detectable in early ne-AMD.[12]

These parameters may play an important role in defining the features of early AMD and its progression.[13] The relationship between functional and anatomic parameters in early AMD and potentially predictive parameters for the progression of disease currently remain unclear.[18,19]

The main goal of this retrospective study was to evaluate the relationship between the morphological changes in early and intermediated ne-AMD, as assessed by OCT examination, and macular functions, based on visual acuity and fERG parameters. The correlations were evaluated by either cross-sectional or longitudinal analyses. In the latter, the potential predictive value of morphological and functional parameters on disease progression was also evaluated.

Methods

Subjects

In this study, we evaluated 141 eyes of 74 patients who underwent treatment at the retina services of the Ophthalmology Unit at the Fondazione Policlinico Universitario A. Gemelli IRCCS, Rome, Italy. All patients were affected by early or intermediate ne-AMD. All patients underwent the following examinations at the same session: (1) best-corrected visual acuity (BCVA), (2) fERG examination, and (3) macular OCT examination. Patients with previous or new diagnoses of neovascular exudative AMD (e-AMD), patients whose eyes presented a signal strength of <5 at the OCT examination, and patients who missed one of the three main examinations at the same session were excluded from the study. Other exclusion criteria were patients affected by other retinal or optic nerve disorders, such as previous retinal detachment, retinal vein or artery occlusion, or glaucoma. One eye for each patient was considered for data analysis. When both eyes had a comparable disease stage, we collected data from the eye with the worse BCVA.

Visual Function Test Methods

All patients diagnosed with ne-AMD underwent a complete ophthalmologic examination, BCVA

Downloaded from tvst.arvojournals.org on 04/22/2022

measurement, fundus stereoscopic evaluation with slit-lamp biomicroscopy, OCT, and fERG examination.[14] The visual acuity of all patients was evaluated before the other functional and structural examinations. Visual acuity was based on the smallest line correctly identified, and the decimal scores were converted to logMAR using the formula logMAR = –log(decimal acuity).[15] The use of Early Treatment Diabetic Retinopathy Study (ETDRS) charts is superior and more accurate compared with Snellen decimal acuity. However, all patients were tested for Snellen acuity, whereas only some patients were also tested with ETDRS charts. For uniformity, we converted all of the Snellen data to logMAR values.

All patients underwent a fERG examination at the same session, and the cone-mediated focal macular ERG testing was executed using a previously published technique.[16] Briefly, fERGs were recorded from the central 18° using a uniform red field stimulus superimposed on an equiluminant steady-adapting background to minimize stray light.

The stimulus was generated by a circular array of eight red light-emitting diodes (LEDs) (K maximum, 660 nm; mean luminance, 93 cd/m^2) presented on the rear of a Ganzfeld bowl (white-adapting background with luminance of 40 cd/m^2). A diffusing filter in front of the LED array made it appear as a uniform field of red light, with the white-adapting background with luminance of 40 cd/m^2. fERGs were recorded in response to the sinusoidal 95% luminance modulation of the central red field. Flickering frequency was 41 Hz. Patients fixated monocularly at a 0.25° central fixation mark under the constant monitoring of an external observer. Subjects underwent a preadaptation period of 20 minutes to the stimulus mean illuminance. fERGs were recorded by an Ag–AgCl electrode taped on the skin over the lower eyelid. A similar electrode, placed over the eyelid of the contralateral patched eye, was used as a reference (interocular recording).

fERG signals were amplified (100,000-fold), bandpass filtered between 1 and 100 Hz (6 decibels/octave), and averaged (12-bit resolution, 2-kHz sampling rate, 200–600 repetitions in two to six blocks). Offline discrete Fourier transform analysis quantified the peak-to-peak amplitude and phase lag of the response fundamental harmonic (first harmonic) at 41 Hz. A noise response at 41 Hz was estimated either by recording the signals in response to an occluded stimulus or by sampling the signal at a frequency 1.1 times the frequency of the stimulation. The noise value at 41 Hz was typically 0.05.

Imaging Assessment

The OCT examination allows specific layers impacted by a disease process to be selectively evaluated. For eyes with ne-AMD, visualization of the individual outer retinal layers has allowed the detection of subtle alterations before they can be identified by color fundus photography or fundus autofluorescence.[9,17] A major morphological parameter evaluated by automated OCT algorithm analysis is the subretinal illumination (SRI) areas in the macular region, identified as bright areas of increased light transmission beneath the RPE corresponding to RPE atrophy over a circular area of 5 mm around the fovea.

For the OCT examination, at least one high-definition 5-line raster image and one 6 × 6-mm macular cube 512 × 128 scan were required. The high-definition 5-line raster and 6 × 6-mm macular cube 512 × 128 scan protocols were performed using OCT (Cirrus HD-OCT 5000 with AngioPlex software, version 10.0; Carl Zeiss Meditec, Jena, Germany).

The parameters examined by OCT to provide structural data for the functional analyses included the following: (1) foveal ONL thickness, (2) EZ interruption, (3) presence or absence of macular drusen or pseudodrusen, and (4) SRI that quantified the RORA and was detected by the device.

Two separate examiners (S.F. and A.S.), based on B-scans through the fovea, manually measured the foveal ONL thickness. The average of their two measures was taken as the final value. When atrophy occurred, the value of 0 was considered. The same two independent retinal operators also manually measured the EZ interruption on the B-scans. The EZ was considered to be the second hyperreflective band on the OCT scan, referring to the inner/outer segment junction of photoreceptors. When multiple EZ interruptions were observed, the nearest interruption to the foveal center was taken as the best assessment (Fig. 1). The consensus agreement (Cohen coefficient agreement) was considered suitable only if >0.9.

The presence or absence of drusen or reticular pseudodrusen was also analyzed by OCT B-scans. Drusen were considered to be deposits between the RPE and Bruch's membrane or pigmentary abnormalities, whereas reticular pseudodrusen were rectangular or pyramidal-shaped foci extending radially through photoreceptor cell-attributable bands.[4] The value of 0 indicated that both were absent, the value of 1 indicated the presence of drusen, and the value of 2 indicated the presence of reticular pseudodrusen. The RORA corresponded to SRI that was automatically measured by the advanced RPE analysis software through the 6 × 6-mm macular cube 512 × 128 images. The advanced

Downloaded from tvst.arvojournals.org on 04/22/2022

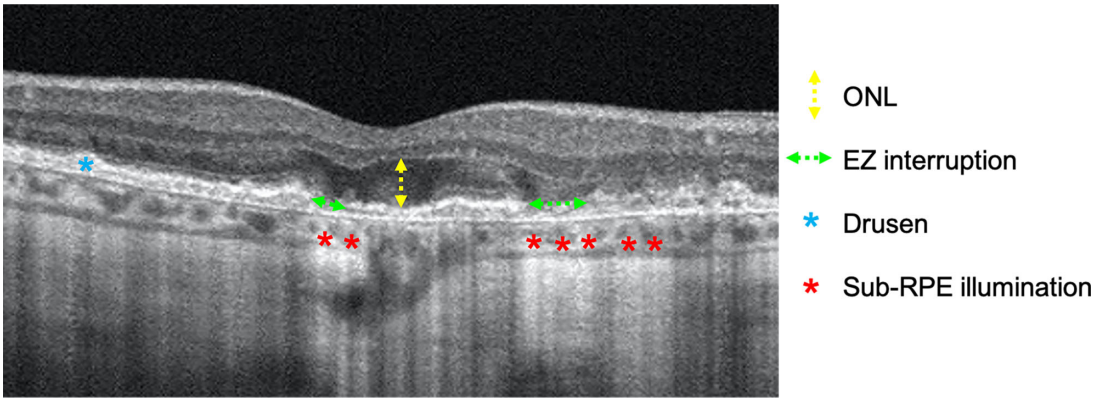

Figure 1. Example of B-scan analysis. The ONL thickness (*yellow arrow*) was assessed in the foveal region; EZ interruption (*green arrows*) was assessed in to the 5 mm around the foveal region as the presence of drusen (*blue asterisks*) or pseudodrusen. Subretinal pigment epithelium transmission (*red asterisks*) was automatically measured by the advanced RPE analysis software embedded in the OCT device.

RPE analysis software was used to determine the areas of SRI (mm^2) for increased light penetration through atrophic RPE and choriocapillaris by means of sub-RPE slab tools derived from segmentation.[13] The SRI identifies bright areas of increased light transmission beneath the RPE, indicating RPE atrophy, and is averaged over a circular area of 5 mm around the fovea by the automated OCT software as previously reported.[13] The automated software provides two types of values: (1) the average of the total SRI area in a circle of 5 mm centered on the fovea, and (2) the closest distance to the fovea in millimeters. For this second measurement, we considered the value to be 0 when the software provided the value of *xxx*, indicating that 0 was the distance from the fovea.

The foveal center on the OCT fundus image was identified using an automated fovea localization algorithm. When the algorithm failed due to significant tissue disruption, the fovea was identified manually. OCT scans passing through the fovea identified clear evidence of zones of light hypertransmission within the choroid corresponding to the retinal pigment epithelium or outer retina atrophy. We used the definition suggested by Guymer et al.,[10] based on OCT-specific findings, to define iRORA or cRORA in our study.

Statistical Analysis

The results from only one eye for each patient (the eye with lower visual acuity or, if acuity was identical in both eyes, the right eye) were included in the analyses. In the cross-sectional part of the study, morphological and functional parameters were correlated in the study eyes. In the longitudinal analysis, results obtained at baseline were compared with those obtained at the end of 12-month follow-up. The cross-sectional study power analysis with Pearson's correlation showed that a sample of 74 patients provided a power of 80% at 0.05 sensitivity to detect a correlation with an r of 0.3. In the longitudinal study, a sample of 34 patients provided a power of 80% at 0.05 sensitivity to detect a change of at least 20% in each numerical parameter at the end of the follow-up. Results were analyzed with non-parametric Mann–Whitney tests or parametric paired t-tests, depending on data distribution.

In the longitudinal study, each studied eye was identified as progressor or non-progressor during follow-up based on the following features:

- Increase in the number of drusen and/or pseudoreticular drusen, and/or
- Increase in RORA area measured in the fovea and in the perifoveal regions (within 5 mm radius from the fovea)

Baseline morphological and functional features were statistically evaluated to determine if one or more parameters differed significantly between "progressor" and "non-progressor eyes." For this analysis, non-parametric Mann–Whitney tests were employed; for the significant parameters, receiver operating characteristic (ROC) curves were analyzed. In the cross-sectional analysis, correlations between morphological and functional parameters were evaluated by Pearson's test. The association between fERG amplitude and drusen type was evaluated by the non-parametric Mann–Whitney test. In the longitudinal analysis, paired t-tests were employed to compare the data collected at baseline with those obtained at 1 year.

Downloaded from tvst.arvojournals.org on 04/22/2022

Results

Cross-Sectional Analysis

BCVA was positively correlated with ONL thickness ($P < 0.001$; $R^2 = 0.24$) and with fERG ($P < 0.001$; $R^2 = 0.20$) and negatively correlated with EZ interruption ($P < 0.001$; $R^2 = 0.38$) and SRI (RORA) area ($P = 0.002$; $R^2 = 0.14$) (Fig. 2). Furthermore, negative correlations between fERG amplitude and SRI parameter ($P = 0.006$; $F = 0.17$) and between fERG amplitude and EZ interruption ($P = 0.01$; $R^2 = 0.10$) were found, indicating deterioration of the ERG response as the severity of damage to the photoreceptor–RPE complex increased (Fig. 3). The fERG amplitude tended to be lower in eyes with reticular pseudodrusen compared with the other two groups. However, due to the large overlap between groups, the difference did not reach statistical significance ($P = 0.13$; $F = 2.19$) (Fig. 4).

Longitudinal Analysis

Thirty-four patients had a follow-up of 12 months, and nine out of the 34 patients showed AMD lesion progression in the studied eye based on the above criteria (see Methods). The remaining 25 patients had no morphological changes over the follow-up period. Figure 5 shows the OCT images in two representative patients having either an appearance of newly formed drusen or an enlargement of the RORA area at the 12-month follow-up.

On average, fERG amplitudes and outer retinal thickness tended to decrease by 15% and 18%, respectively, after 1-year follow-up. These changes did not differ between eyes with anatomic disease progression and those not showing any change. The decline was not statistically significant, with the mean fERG amplitude being 0.68 ± 024 at baseline and 0.54 ± 0.22 at 1 year; the mean outer retinal thickness at baseline was 45 ± 12 µm, and at 1 year it was 38 ± 12 µm (paired t-test = 0.43).

Among the examined parameters, RORA area at baseline significantly predicted the anatomic progression of the AMD lesions after 1 year. Indeed, the median RORA area was larger in progressor compared with non-progressor eyes. Using a cutoff of 1.5 mm, ROC curve analysis showed a sensitivity of 81.8%, a specificity of 36.4%, and a total accuracy of 77% (area under the curve = 0.77) (Fig. 6) to predict ne-AMD progression in our studied eyes. The Table shows the dataset of involved eyes.

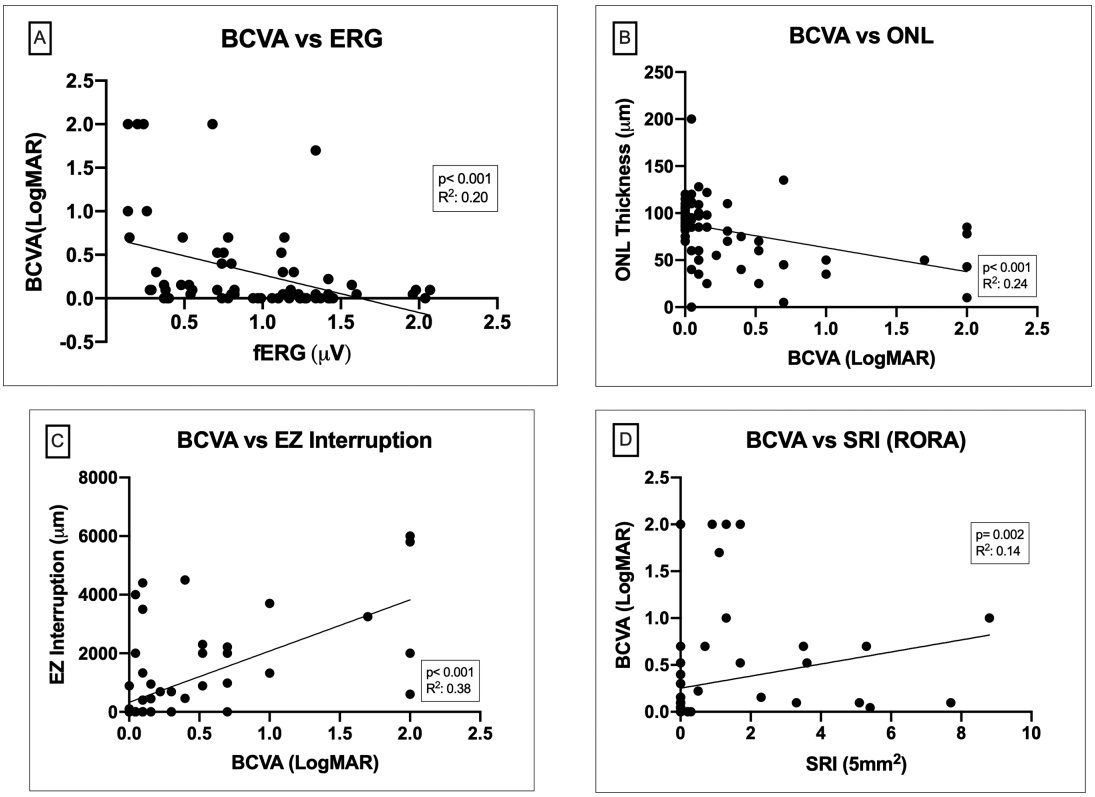

Figure 2. The values of BCVA plotted as a function of morphological parameters are shown. BCVA was positively correlated with ONL thickness ($P < 0.001$) and fERG amplitude ($P < 0.001$), and BCVA was negatively correlated with EZ interruption ($P < 0.001$) and SRI (RORA) area ($P = 0.002$).

Downloaded from tvst.arvojournals.org on 04/22/2022

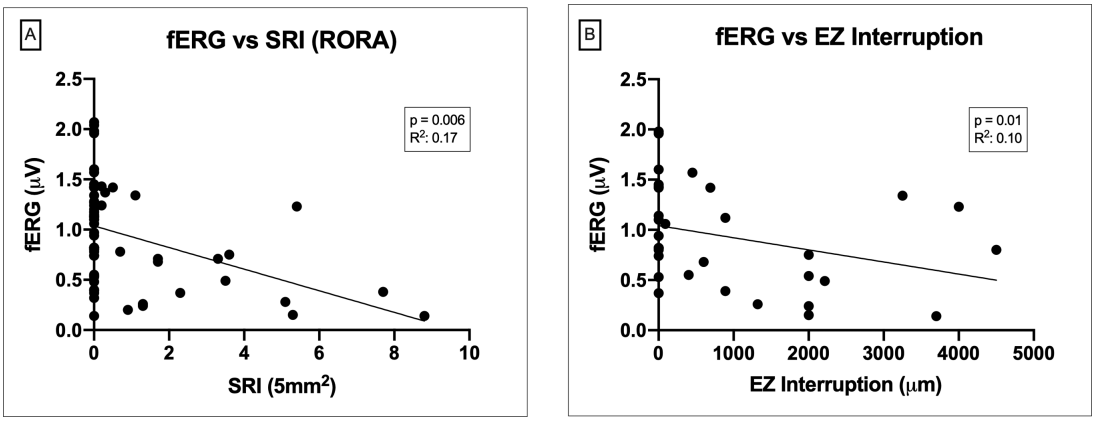

Figure 3. The values of fERG amplitude plotted as a function of the SRI (RORA) area are shown. The negative correlations between fERG amplitude and SRI parameter ($P = 0.006$) and EZ interruption ($P = 0.01$) suggest a deterioration of the fERG response with an increase in the severity of damage to the photoreceptor–RPE complex (SRI).

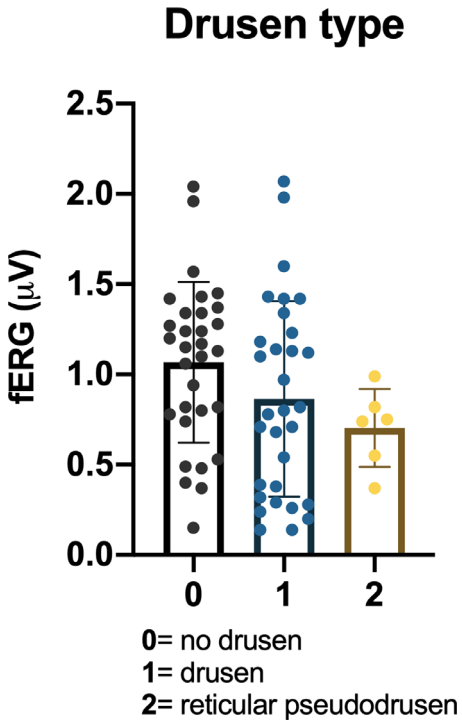

Figure 4. The box plots show the fERG amplitude values as a function of presence or absence of drusen as well as drusen type (drusen or reticular pseudodrusen). fERG amplitude tended to be lower in eyes with reticular pseudodrusen compared with the drusen or no drusen group. The difference was not statistically significant ($P = 0.13$; $F = 2.19$) because the groups overlapped largely.

Discussion

Our study was designed to evaluate the correlation between functional and morphologic parameters in early and intermediate AMD. The correlation was evaluated both cross-sectionally and longitudinally. The main hypothesis was that the structure–function relation may help for early diagnosis of ne-AMD lesions and for predicting their progression in a short-term follow-up. The results showed that microanatomic abnormalities of the macula were correlated with abnormalities in functional parameters (acuity, fERG), indicating early losses in retinal function.[13,21] In addition, the extent of RORA, a parameter correlated with visual acuity and fERG amplitude, significantly predicted the progression of disease at 12 months. Our findings support the diagnostic power and predictivity of morphofunctional assessments in ne-AMD eyes.

Our previous studies reported that, in early ne-AMD patients with soft drusen and/or early RPE defects, fERG could detect a loss of retinal flicker sensitivity and response kinetics in eyes with normal visual acuity.[13] In addition, the abnormalities of the fERG response tended to be more profound and severe as the AMD lesions became more severe.[11,14] In other studies, the combination of microperimetric sensitivity and low luminance deficit assessment have been reported as suboptimal in predicting the progression of disease.[21]

Morphologically, according to the AREDS study, drusen and pigmentary changes identified on color fundus photography are considered diagnostic signs of early and intermediate age-related macular degeneration.[3] Subsequent identification of reticular pseudodrusen and subretinal drusenoid deposits indicated that they were the main cause of ne-AMD progression to exudative forms.[6] An important role is also played by autofluorescence (not evaluated in the current study), especially quantitative autofluorescence, which has shown signal declines with progression to atrophy.[22] The use of this method is relevant when conducting

Downloaded from tvst.arvojournals.org on 04/22/2022

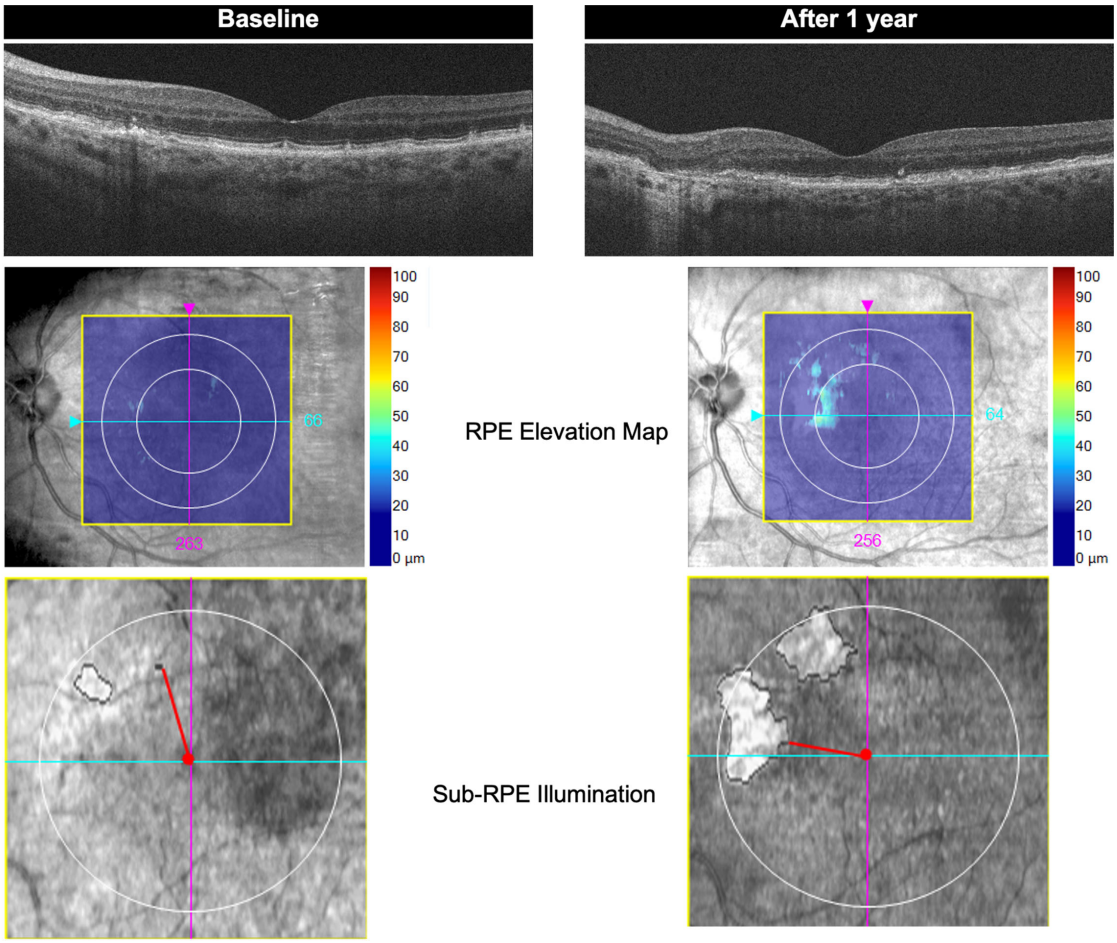

Figure 5. Morphological changes of one representative subject and presenting the findings at baseline and after 1 year. At baseline, the B-scan shows the pseudodrusen (pyramidal-shaped foci that extend radially through the photoreceptor layer) that result in greater irregularity after 1 year. Additionally, the RPE elevation map shows the growth of irregularity, and the sub-RPE illumination analysis indicates the progression of RORA.

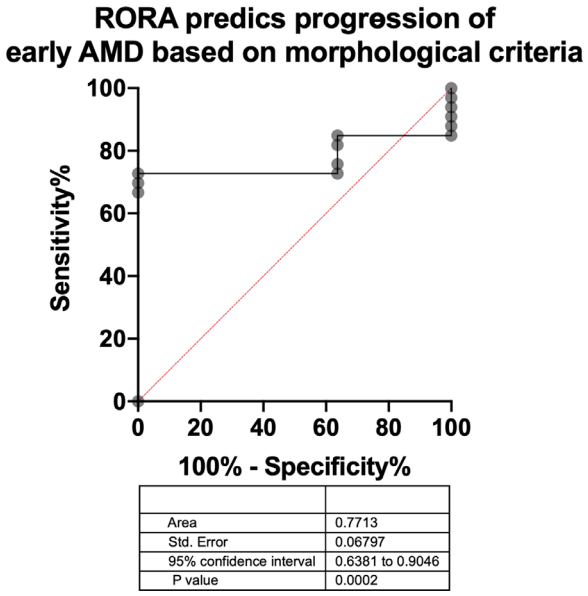

Figure 6. ROC curve showing a sensitivity of 81.8%, a specificity of 36.4%, and a total accuracy of 77% (area under the curve = 0.77) to predict ne-AMD progression in the studied eyes.

longitudinal observation[23] and should be applied in future structure–function studies in ne-AMD.[24]

Recently, morphological features observed by RORA have been described as potential biomarkers for the evaluation of eyes with ne-AMD mainly in early and intermediate stage.[10,13] The SRI represents a quantitative index (expressed in mm^2) of either iRORA or cRORA, with respect to the 250-µm-width cutoff used to discriminate between the two stages of AMD.[9] The measurement obtained by SRI analysis corresponded to the total area of light hypertransmission through the choroid due to the atrophy of RPE and outer retina. Hence, the introduction of RORA added much information about the integrity of the RPE. The SRI is an objective morphological parameter for the evaluation of RORA during the follow-up of eyes with RPE disturbances, such as ne-AMD. Visual acuity and fERG amplitude were correlated ($P < 0.01$) with RORA area.

In this study, we considered the potential predictivity of fERG and RORA in ne-AMD eyes. Our results

translational vision science & technology

Downloaded from tvst.arvojournals.org on 04/22/2022

Table. Sensitivity and Specificity of the RORA Area to Predict Morphologic Progression of AMD in Studied Eyes

	Sensitivity %	95% CI	Specificity %	95% CI	Likehood Ratio
<1.200	75.76	58.98% to 87.17%	36.36	22.19% to 53.38%	1.190
<1.500	81.82	65.61% to 91.39%	36.36	22.19% to 53.38%	1.286

show that fERG amplitude was correlated ($P < 0.01$) with the extent of EZ interruption and tended to be lower in reticular pseudodrusen compared with the soft drusen eyes. Furthermore, in the longitudinal analysis, both fERG amplitudes and outer retinal thickness tended to decrease after a 1-year follow-up (on average by 15% and 18%, respectively), although these changes, due to a small sample size, did not reach statistical significance. An important aspect of our results is that baseline RORA area, but not fERG amplitude or visual acuity, significantly predicted (with 77% accuracy, $P < 0.01$) morphological deterioration after 1 year. These findings suggest that SRI should be evaluated regularly at baseline in clinical practice to predict the evolution of damage with greater accuracy to better personalize treatment.

In conclusion, our results show that assessment of functional visual acuity can detect morphological abnormalities in early and intermediate AMD eyes. SRI reflected the presence of RORA, a potential predictor of AMD lesion progression, in a short-term follow-up, prompting further longitudinal studies in ne-AMD to confirm this hypothesis.

Acknowledgments

The authors thank Franziska Michaela Lohmeyer for her English editing service.

Disclosure: **M.C. Savastano**, None; **B. Falsini**, None; **S. Ferrara**, None; **A. Scampoli**, None; **M. Piccardi**, None; **A. Savastano**, None; **S. Rizzo**, None

[*] MCS and BF equally contributed in the realization of this article.

References

1. Rosenblatt TR, Vail D, Saroj N, Boucher N, Moshfeghi DM, Moshfeghi AA. Increasing incidence and prevalence of common retinal diseases in retina practices across the United States. *Ophthalmic Surg Lasers Imaging Retina*. 2021;52(1):29–36.
2. Schmitz-Valckenberg S, Alten F, Steinberg JS, et al. Reticular drusen associated with geographic atrophy in age-related macular degeneration. *Invest Ophthalmol Vis Sci*. 2011;52(9):5009–5015.
3. Age-Related Eye Disease Study Research Group. The Age-Related Eye Disease Study system for classifying age-related macular degeneration from stereoscopic color fundus photographs: the Age-Related Eye Disease Study Report number 6. *Am J Ophthalmol*. 2001;132(5):668–681.
4. Zweifel SA, Imamura Y, Spaide TC, Fujiwara T, Spaide RF. Prevalence and significance of subretinal drusenoid deposits (reticular pseudodrusen) in age-related macular degeneration. *Ophthalmology*. 2010;117(9):1775–1781.
5. Jhingan M, Singh SR, Samanta A, et al. Drusen ooze: predictor for progression of dry age-related macular degeneration. *Graefes Arch Clin Exp Ophthalmol*. 2021;259(9):2687–2694.
6. Nassisi M, Lei J, Abdelfattah NS, et al. OCT risk factors for development of late age-related macular degeneration in the fellow eyes of patients enrolled in the HARBOR study. *Ophthalmology*. 2019;126(12):1667–1674.
7. Cicinelli MV, Rabiolo A, Sacconi R, et al. Retinal vascular alterations in reticular pseudodrusen with and without outer retinal atrophy assessed by optical coherence tomography angiography. *Br J Ophthalmol*. 2018;102(9):1192–1198.
8. Ferris FL, Wilkinson CP, Bird A, et al. Clinical classification of age-related macular degeneration. *Ophthalmology*. 2013;120(4):844–851.
9. Sadda SR, Guymer R, Holz FG, et al. Consensus definition for atrophy associated with age-related macular degeneration on OCT: Classification of Atrophy Report 3. *Ophthalmology*. 2018;125(4):537–548.
10. Guymer RH, Rosenfeld PJ, Curcio CA, et al. Incomplete retinal pigment epithelial and outer retinal atrophy in age-related macular degeneration: Classification of Atrophy Meeting Report 4. *Ophthalmology*. 2020;127(3):394–409.
11. Falsini B, Fadda A, Iarossi G, et al. Retinal sensitivity to flicker modulation: reduced by early age-related maculopathy. *Invest Ophthalmol Vis Sci*. 2000;41(6):1498–1506.

Downloaded from tvst.arvojournals.org on 04/22/2022

12. Capoluongo E, Concolino P, Piccardi M, et al. Retinal function and CFH-ARMS2 polymorphisms analysis: a pilot study in Italian AMD patients. *Neurobiol Aging*. 2012;33(8):1852.e5–1852.e12.
13. Savastano MC, Falsini B, Cozzupoli GM, et al. Retinal pigment epithelial and outer retinal atrophy in age-related macular degeneration: correlation with macular function. *J Clin Med*. 2020;9(9):2973.
14. Falsini B, Serrao S, Fadda A, et al. Focal electroretinograms and fundus appearance in nonexudative age-related macular degeneration. Quantitative relationship between retinal morphology and function. *Graefes Arch Clin Exp Ophthalmol*. 1999;237(3):193–200.
15. Mataftsi A, Koutsimpogeorgos D, Brazitikos P, Ziakas N, Haidich AB. Is conversion of decimal visual acuity measurements to logMAR values reliable? *Graefes Arch Clin Exp Ophthalmol*. 2019;257(7):1513–1517.
16. Galli-Resta L, Piccardi M, Ziccardi L, et al. Early detection of central visual function decline in cone-rod dystrophy by the use of macular focal cone electroretinogram. *Invest Ophthalmol Vis Sci*. 2013;54(10):6560–6569.
17. Wu Z, Luu CD, Ayton LN, et al. Optical coherence tomography-defined changes preceding the development of drusen-associated atrophy in age-related macular degeneration. *Ophthalmology*. 2014;121(12):2415–2422.
18. Guymer R, Wu Z. Age-related macular degeneration (AMD): more than meets the eye. The role of multimodal imaging in today's management of AMD-A review. *Clin Exp Ophthalmol*. 2020;48(7):983–995.
19. Somasundaran S, Constable IJ, Mellough CB, Carvalho LS. Retinal pigment epithelium and age-related macular degeneration: a review of major disease mechanisms. *Clin Exp Ophthalmol*. 2020;48(8):1043–1056.
20. de Jong S, Gagliardi G, Garanto A, et al. Implications of genetic variation in the complement system in age-related macular degeneration. *Prog Retin Eye Res*. 2021;84:100952.
21. Minnella AM, Piccardi M, Placidi G, et al. Macular function in early and intermediate age-related macular degeneration: correlation with the Simplified Thea Risk Assessment Scale (STARS). *Transl Vis Sci Technol*. 2020;9(10):28.
22. Wu Z, Luu CD, Hodgson LA, et al. Examining the added value of microperimetry and low luminance deficit for predicting progression in age-related macular degeneration. *Br J Ophthalmol*. 2021;105(5):711–715.
23. Reiter GS, Hacker V, Told R, et al. Longitudinal changes in quantitative autofluorescence during progression from intermediate to late age-related macular degeneration. *Retina*. 2021;41(6):1236–1241.
24. Reiter GS, Told R, Baratsits M, et al. Repeatability and reliability of quantitative fundus autofluorescence imaging in patients with early and intermediate age-related macular degeneration. *Acta Ophthalmol*. 2019;97(4):e526–e532.

Downloaded from tvst.arvojournals.org on 04/22/2022